CHARACTERISTICS OF X-RAY COMPUTER TOMOGRAPHY APPLICATION TO COMPOSITE MATERIAL RESEARCH

V. I. Barakhov, V. A. Chernyaeva, and V. S. Kiselev

UDC 541.18+539.217.1

The article deals with characteristics of tomography associated with the interaction of X radiation with a material, mathematical scan processing, and random errors in determination of linear attenuation coefficients.

X-ray computer tomography (XCT) occupies a special place in composite material research. Its unique capabilities that cannot be offered by any other method are used in studying the composite macrostructure, estimation of volume contents of material components, determination of changes in the structural parameters induced by various external actions, in refining production methods, seeking relations between the physico-mechanical properties and the structure parameters, describing the physical aspect of such processes as heat and mass transfer, and estimation of the process characteristics, in development and creation of new materials, and in testing the product's quality. High metrological characteristics, great functional capabilities, and a large amount of information on the object structure and state can raise the composite research to a qualitatively new level. The method makes it possible to estimate the density of every elementary cell of the material specimen without destroying its integrity during experiments. Because of its short wavelength, X radiation has a large penetrating ability, and therefore even at energies as low as 100 keV it can be applied to specimens of nearly all modern composite materials: glass-reinforced plastics, organoplastics, carbon-filled plastics, carbon-carbon composites and their hybrids in a wide thickness range. Like any other method, XCT has its own characteristics that should be taken into account while using the technique. We will discuss two aspects of these characteristics: the first is associated with the specificity of the method itself, the second with its metrological capabilities.

Specificity of XCT needs consideration of the properties of X radiation, interaction with the material, photon fixing before and after passing through the matrial, and mathematical processing of scans involving the image restoration from projections. Unlike optical spectra, X-ray spectra involve electron transitions in the inner atomic shells (but not in the outer valences), they are simple, similar for different elements, depend on the charge of the nucleus, and independent of the physical composition of the material. X radiation incident on the material gives rise to three main actions [1].

1. The photoelectric effect is a process in which a photon with the energy E_0 transfers the energy to an electron within the atomic shell. After that, the electron moves to a higher level, or if the photon energy exceeds the electron binding energy in the atom, it leaves the atom. The photoelectric absorbance (τ) depends on the ordinal number z of the absorbing atoms and the radiation wavelength λ. Since $\tau \sim z^3\lambda^3$, this process is of key importance when radiation energies smaller than 0.3 to 0.5 MeV are used and materials with a large z are examined.

2. Photon scattering (σ_s) is a process in which radiation attenuates because of the deflection of photons colliding with electrons of the absorbing material atoms. It may occur with or without changing their wavelengths and energy. Compton scattering is photon scattering in which both the photon direction and the wavelength change. Some of the energy is therewith transferred to the electron (the Compton effect). The Compton scattering attenuation coefficient is proportional to the ordinal number z of the absorbing material atoms. It is substantial when using shortwave ($\lambda < 0.03$ nm) radiation, and dominates for elements with $z < 30$ with a quantum energy of 0.3 to 1.0 MeV.

Coherent scattering is photon scattering on the atoms without energy change. It can be observed at a low photon energy and comparatively more substantial electron binding energy.

3. Formation of electron-positron pairs ($\varkappa$) can take place at quantum energies higher than 1.022 MeV.

Translated from Inzhenerno-fizicheskii Zhurnal, Vol. 63, No. 6, pp. 744-751, December, 1992. Original article submitted November 28, 1991.

1062-1025/92/6306-1249$12.50

TABLE 1. LAC of Some Binders and Fillers for the SOMATOM DR-2 X-Ray Tube

	Density, $\rho \times 10^3$, kg/cm^3	Operating conditions of the tube			
		125 kV, 780 mA·sec		96 kV, 1000 mA·sec	
		$F \cdot 10^{-2}$, 1/m	f	$F \cdot 10^{-2}$, 1/m	f
Glass	2,607	0,586	2114,3	0,662	2345,5
EDT-10	1,209	0,224	193,2	0,237	195,9
EKhD-MK	1,260	0,241	284,0	0,258	307,4
EKhD-U	1,334	0,280	490,6	0,309	560,5
Compound	1,205	0,230	220,7	0,224	232,1
UUKM*	1,910	0,317	687,0	0,330	671,0
UUKM*	1,950	0,329	752,0	0,334	736,0

*UUKM is the carbon-carbon composite material with different packings.

Many composites were studied on a SOMATOM DR-2 tomograph with an X-ray tube operating at energies under ~ 100 keV. In this case the main contribution to the linear attenuation coefficient (LAC) is made by the photoelectric effect. The component σ_s is less significant, $\varkappa = 0$. The total LAC is the sum of the attenuation coefficients τ and σ_s:

$$F = \tau + \sigma_s. \tag{1}$$

The LAC matrices transformed into tomographic images of the scanned objects are prescribed in the Hounсefield scale. In terms of the Hounсefield to ordinary LAC ratio we can find

$$f = \left(\frac{F}{F_w} - 1\right) \cdot 1000. \tag{2}$$

In the XCT examination of composites, the change to density matrices from LAC matrices is an important point. In this case, it is a separate problem to be solved, taking the interaction of X radiation with the material, the mathematical characteristics of the image restoration from projections, and the scaling of LAC values into account. The relation between the density and LAC can be found from the following considerations.

The joint effect of X-ray scattering and absorption described above results in exponential attenuation of a photon beam as it passes through the material specimen

$$I = I_0 \exp\left[-\int_A^B f(x, y)\, dy\right]; \quad I = I_0 \exp(-\sigma n_a h); \tag{3}$$

$$n_a = \frac{N_A \rho}{A}. \tag{4}$$

Generalization of (3) and (4) gives

$$F = \frac{N_A \sigma \rho}{A}, \tag{5}$$

and hence it follows that the LAC of a material is proportional to its density and depends on its chemical composition. Substituting (5) for the material and water into (2) gives

$$\rho = \rho_w \frac{\sigma_w A}{\sigma A_w}(1 + 0{,}001 f). \tag{6}$$

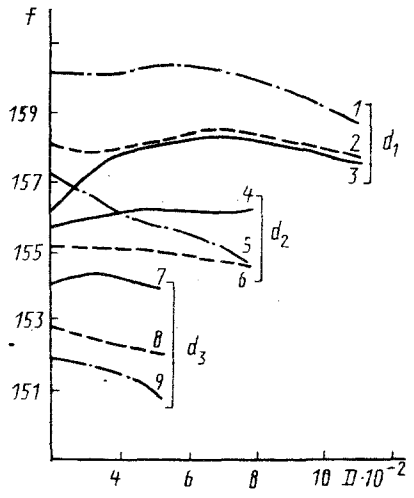

Fig. 1

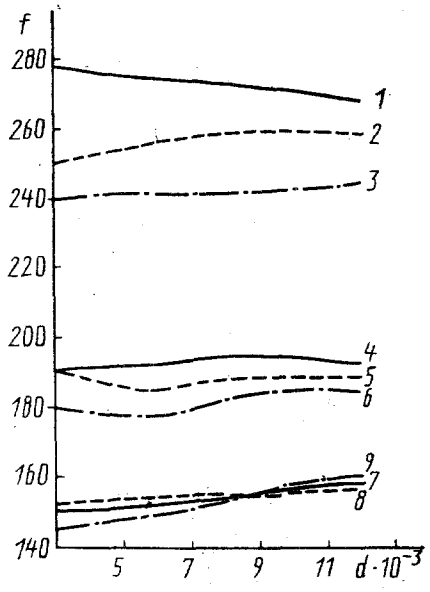

Fig. 2

Fig. 1. Plot of LAC of the ÉDT-10 binder of various sizes (diameters d = $12 \cdot 10^{-3}$ m, d = $9 \cdot 10^{-3}$ m, d = $6 \cdot 10^{-3}$ m) versus the diameters of the zone of interest under different X-ray tube operating conditions. 3, 4, 7) 85 kV, 1280 mA·sec; 2, 6, 8) 96 kV, 1000 mA-sec; 1, 5, 9) 125 kV, 780 mA·sec. $D \cdot 10^{-2}$, m.

Fig. 2. Plot of LAC of the binders versus the specimen diameters for various X-ray tube operating conditions. 1, 4, 7) 85 kV, 1280 mA·sec; 2, 5, 8) 96 kV, 1000 mA·sec; 3, 6, 9) 125 kV, 780 mA·sec.

In order to obtain the density matrices $P(\rho_{x,y})$ from the LAC matrices $F(f_{x,y})$ it is necessary to update formula (6). It should be borne in mind that LAC matrix elements f(x,y) obtained after composite specimen scanning can differ from the true values that are estimated in the following way. It follows from expressions (3) and (5) that the LAC can be determined from

$$F = -\ln \frac{I}{I_0} \frac{1}{h}. \tag{7}$$

It is most likely that the intensities of the incident and transmitted beams can be found from the readings of the tomograph detectors. Naturally, when they are arranged in a semicircle, the readings of one or two of them may only be used. The incident beam intensity (I_0) is evaluated from air scanning and the transmitted beam intensity (I) from scanning of the test material specimen which must be located exactly at the matrix (aperture) center. This should be done for a more exact estimation of the absorber thickness (h). Determination of the LAC for arbitrarily shaped scanned cross sections of the specimen requires an averaged h. Most often they have a cross section in the form of a circle, a square, or a rectangle. When central detectors are used (with SOMATOM 255, 256), for specimens with a circular cross section h = D, where D is the circle diameter. For the other two cross sections h is a function of the rotation angle $h = \eta(\alpha)$ and varies between a and d, where a is the side of a square or the shortest side of a rectangle; d is the diagonal of the square or rectangle. The average absorbent thickness is defined by

$$h_{av} = \frac{\int_0^{\alpha_\ell} \eta(\alpha)\, d\alpha}{\alpha_\ell}. \tag{8}$$

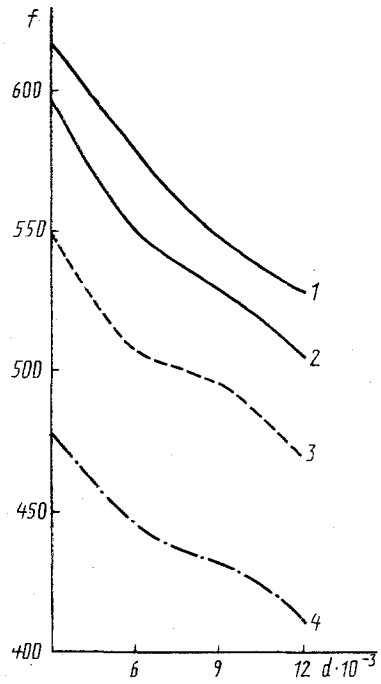

Fig. 3

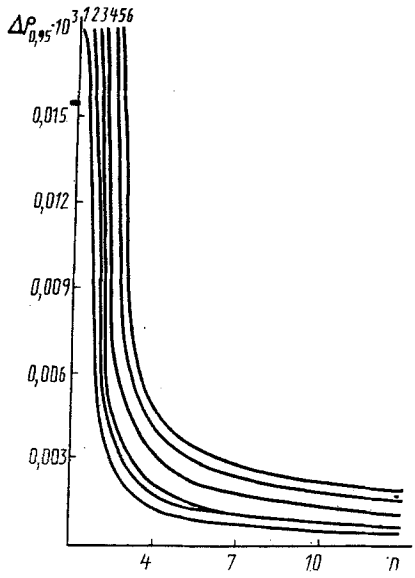

Fig. 4

Fig. 3. Plot of LAC for ÉKhD-U binder [2) 85 kV, 1280 mA·sec; 3) 96 kV, 1000 mA·sec; 4) 125 kV, 780 mA·sec] and $CaCl_2$ solution (1) versus the specimen diameters for different X-ray tube operating conditions.

Fig. 4. Plot of the random errors in the estimated composite densities versus the number of rescans with different numbers of averaging cells. 1) ST = 36.0, N = 50; 2) 36.0 and 30; 3) 36.0 and 10; 4) 6.0 and 1; 5) 36.0 and 1; 6) 42.4 and 1. $\Delta\rho_{0.95}$, kg/m^3.

Formula (8) can be written for particular cases as follows: for a square

$$h_{av} = \frac{4a \ln \operatorname{tg} \frac{3\pi}{8}}{\pi}; \tag{9}$$

for a rectangle

$$h_{av} = \frac{1}{2}\left[\frac{a \ln \operatorname{tg} \frac{\pi + 2 \operatorname{arctg} \frac{b}{a}}{4}}{\operatorname{arctg} \frac{b}{a}} + \frac{b \ln \operatorname{tg}\left(\frac{3\pi}{8} - \frac{\operatorname{arctg} \frac{b}{a}}{2}\right)}{\frac{\pi}{4} - \operatorname{arctg} \frac{b}{a}}\right]. \tag{10}$$

In practical examination of composites, for example, in determination of their compositions, both the material and its components have to be scanned. This is most often a reinforcing filler and a polymer matrix. It is known that if the material consists of N_c components with mass absorption coefficients F_i/ρ_i, then [2]

$$\frac{F}{\rho} = \sum_{i=1}^{N_W} \frac{F_i}{\rho_i} \mu_i^W. \tag{11}$$

Since the relation between the volume and weight fractions is expressed by $\mu_i = \mu_i^w(\rho/\rho_i)$, formula (11) can be written as follows:

$$F = \sum_{i=1}^{N_W} F_i \mu_i; \quad \ln \frac{I}{I_0} \frac{1}{h} = \sum_{i=1}^{N_W} \ln \frac{I_i}{I_0} \frac{1}{h_i} \mu_i. \tag{12}$$

At $h_1 = h_2 = \ldots = h_N = h$, Eq. (12) takes the form

$$\ln I = \sum_{i=1}^{N_C} \ln I_i \mu_i. \tag{13}$$

In Table 1 LAC calculated for particular binders and fillers after scanning on a SOMATOM DR-2 are presented.

For XCT the relation between the density and LAC is not completely reflected by formula (6). As is known, the two-dimensional LAC distribution f(x, y) can be restored from a discrete system of measured radiation attenuation by the test cross section by the formula [3-5]

$$f(x, y) = \int_0^{2\pi} d\varphi \int_0^{\infty} |\omega| P_f(\omega, \varphi) \exp[i2\pi\omega(x \cos\varphi + y \sin\varphi)] d\varphi. \tag{14}$$

On a SOMATOM DR-2 the restoration is done using the inverse projection method with convolution-based filtration. In this case estimate f^* of the function f(x, y) is

$$f^* = R(\dot{P}_{*y} q). \tag{15}$$

If the Radon transform of P = P(s, φ) is assumed to be a certain signal, then the convolution operation is performed in this case by transmitting the signal through the same filter. On a SOMATOM the convolution cores are realized as data modes. A definite convolution core corresponds to every mode. Naturally, they introduce their corrections into the estimated LAC of elementary cells.

Moreover, in cell LAC estimation it is necessary to take into account that the ray path hardness changes as the rays pass through the object. The radiation beam used in tomography consists of different energy photons. Its spectrum contains a large number of energy levels. Since attenuation at a certain point of the space is usually larger in photons with a lower energy, as the radiation passes through the object the spectrum becomes harder. With the changes in the ray path hardness and limitation of the restoration field by the dimensions of a 256 × 256 matrix taken into consideration, it becomes necessary to correct the LAC tomography estimates of LAC for the test specimen dimensions. To generalize the above mentioned, we can write

$$\rho_{ij} = k\rho_w(1 + 0.001 f_{ij}). \tag{16}$$

For particular composites the correlations between the density and LAC are obtained:

$$\text{for UUKM } \rho = 1{,}1697 + 111{,}22 \cdot 10^{-5} \cdot f, \; r = 0.997;$$

$$\text{For carbon-filled plastic } \rho = 1.2091 + 816{,}77 \cdot 10^{-6} \cdot f, \; r = 0{,}934;$$

$$\text{For glass-reinforced plastic } \rho = 1.0960 + 767{,}28 \cdot 10^{-6} \cdot f, \; r = 0{,}926.$$

One can see from the above expressions that the relation between the density and attenuation for composites is close to the functional one. Nearly all tomographic studies of composites are aimed at estimating the density or its changes in local mater-

ial volumes. Therefore, the coefficients of correlation between ρ and f, characterizing the density points, can be a criterion in choosing the data processing and scanning modes.

It seems important to pay attention to the errors in the LAC estimates caused by the sizes of the test specimen and the zone of interest. In Fig. 1 LAC values are plotted versus the diameter of the scanned object with different tomography conditions for the ÉDT-10 binder shaped as disks produced from a single blank by successive turning. One can see from Fig. 1 that as the zone-of-interest size increases, LAC estimates decrease nearly for all operation conditions of the X-ray tube. Changes in LAC and their respective estimation errors are insignificant here. As follows from Fig. 2, the curves of material LAC versus diameters of the scanned specimens have different shapes depending on the radiation beam wavelength spectrum which is presented by the X-ray tube operating conditions and the chemical composition of the test composite. The element composition influences the ray path hardness, redistributing the importance of absorption and scattering effects in every particular case. Scanning materials of different densities and calcium chloride solutions of different concentrations has shown that LAC changes become substantial as the material densities rise (Fig. 3). Analysis of Table 1 and LAC curves in Figs. 1 to 3 shows that the true LAC estimates can be obtained on a tomograph only with the use of a scaling operation.

The feature of XCT application for composite examination associated with the scanning layer thickness choice is described by the present authors in [6].

Now, we consider some metrological feasibilites of XCT, which are characterized by statistical errors in the output characteristics. The errors are conditioned by the quantum structure of the radiation itself, the random process accompanying radiation transmission through the test specimen material, random recording of transmitted radiation, and internal noises of the receiver. They can be lower than a certain prescribed level and are minimized by repeated scans of the same cross section followed by the averaging of the results over several cells.

In order to determine the dependence of the measuring errors on the density, heterogeneity, the numbers of rescans n and of averaged cells N, an experiment was carried out with organoplastic and glass-reinforced plastic specimens. Random errors in the measured LAC will result in similar errors in the estimated densities. They can be found from the formula [7]

$$\Delta\rho_{0,95} = t_{0,95}\frac{S_\rho}{\sqrt{n}}; \tag{17}$$

$$S_\rho = k\rho_w \cdot 0{,}001ST. \tag{18}$$

The calculated random errors in the estimated composite densities for LAC matrices obtained in the experiments with many rescans of organoplastic specimens are given in Fig. 4 as $\Delta\rho_{0.95}$ = f(n) curves at different ST and N. As one can see from the figure, the random error in XCT density primarily depends on the rescan number n and, to a smaller extent, on the number of averaging cells N and the density heterogeneity S_ρ. It should be noted that $\Delta\rho_{0.95}$ decreases substantially as n rises from 1 to 2, 3, 4, or 5 scans per cross section for all N and S_ρ. For glass-reinforced plastic the curves $\Delta\rho_{0.95}$= f(n) nearly coincide with the curves in Fig. 4. Using the data presented here, for the composities considered one can select the appropriate n and N from the condition that the random density measuring error does not exceed the prescribed value.

Apart from the XCT characteristics described above, for a higher acuracy of the output estimates for composites it is necessary to follow the rotation direction, to include the boundary effects with the aid of compensators (see [8]), to prevent artifacts, to thermostat the specimens before scanning, to take into consideration the temperature drift of the measuring channels, and if necessary, to recalculate LAC matrices in order to take account of the errors arising in setting the specimens at a new scanning of the same section.

In conclusion, it is necessary to emphasize that in every particular case of XCT examination of composites it is necessary to make a differentiation between the importance of characteristics depending on the goals of the study and the required accuracy of LAC estimates, and accordingly, to decide about their inclusion.

Thus, the complicated interaction of X radiation with material, mathematical processing of scans, and random errors in LAC estimates form the characteristics of XCT application for composite testing and determine their necessity.

NOTATION

f, linear attenuation coefficient of material (LAC of material) in the Hounсefield scales; F, F_w, LAC of material and water, respectively, in the ordinary scale (1/m); I_0, I, intensities of the incident and transmitted beams; σ, atomic coefficient

of a narrow radiation quantum beam attenuation (m^2); h, the total absorber thickness; n, the atom number in unit volume; N_A, Avogadro number; A, atomic mass of absorbing material; ρ, material density; α_l, the upper limit of the angle α; b, the larger side of the rectangle; μ_i^w, weight fraction of the i-th element; $P_F(\omega, \varphi)$, one-dimensional transform of the Fourier function $P(s, \varphi)$ for the variable s; R, the Radon transformation operator; xy, convolution operator of the first variable; q, the convolution function or the convolution core; k, proportionality factor depending on the data mode, chemical composition of material, radiation energy, scanned specimen size; r, the coefficient of correlation between the density and LAC; $t_{0.95}$, the Student distribution quantile for a bilateral symmetrical confidence interval with the confidential probability $P = 0.95$; S_ρ, estimated root mean square deviation of density; ST, estimated root mean square deviation of LAC.

REFERENCES

1. S. V. Rumyantsev, A. S. Shtan', and Yu. F. Popov, Roentgeno- and Gamma-Defectoscopist's Handbook [in Russian], Moscow (1969).
2. N. G. Gusev, L. R. Kimel', and V. P. Magikovich, Physical Fundamentals of Radiation Shielding [in Russian], Moscow (1969).
3. G. Hermen, Projection Restoration of Images. Fundamentals of Restoration Tomography [Russian translation], Moscow (1983).
4. I. N. Troitskii, Statistical Theory of Tomography [in Russian], Moscow (1989).
5. A. Makowski, Tr. Inst. Istor. Éstestvozn. Tekh., Akad. Nauk SSSR, **71**, No. 3, 104-111 (1983).
6. V. I. Barakhov, V. A. Chernyaeva, V. S. Kiselev, and A. P. Stepanov, Inzh.-fiz. Zh., **55**, No. 6, 927-929 (1988).
7. P. V. Novitskii and I. A. Zograf, Estimation of Measurement Errors [in Russian], Moscow (1991).
8. V. I. Barakhov, V. A. Chernyaeva, A. P. Stepanov, and V. S. Kiselev, Defektoskopiya, No. 6, 8-12 (1989).